

Density-functional investigation of the rhombohedral to simple cubic phase transition of arsenic

Patricia Silas,¹ Jonathan R. Yates,¹ and Peter D. Haynes²

¹*Theory of Condensed Matter, Cavendish Laboratory, University of Cambridge,
JJ Thomson Avenue, Cambridge CB3 0HE, United Kingdom*

²*Departments of Materials and Physics, Imperial College London,
Exhibition Road, London SW7 2AZ, United Kingdom*

(Dated: February 2, 2022)

We report on our investigation of the crystal structure of arsenic under compression, focusing primarily on the pressure-induced A7 \rightarrow simple cubic (sc) phase transition. The two-atom rhombohedral unit cell is subjected to pressures ranging from 0 GPa to 200 GPa; for each given pressure, cell lengths and angles, as well as atomic positions, are allowed to vary until the fully relaxed structure is obtained. We find that the nearest and next-nearest neighbor distances give the clearest indication of the occurrence of a structural phase transition. Calculations are performed using the local density approximation (LDA) and the PBE and PW91 generalized gradient approximations (GGA-PBE and GGA-PW91) for the exchange-correlation functional. The A7 \rightarrow sc transition is found to occur at 21 ± 1 GPa in the LDA, at 28 ± 1 GPa in the GGA-PBE and at 29 ± 1 GPa in the GGA-PW91; no volume discontinuity is observed across the transition in any of the three cases. We use k -point grids as dense as $66 \times 66 \times 66$ to enable us to present reliably converged results for the A7 \rightarrow sc transition of arsenic.

I. INTRODUCTION

It is currently de rigueur to examine, both experimentally and theoretically, the structure of materials subjected to extremely high pressures.¹ The group-V semi-metals, which include arsenic, are of particular interest as they all exhibit a distinctive low-symmetry structure when uncompressed. With pressure, these elements experience transitions into structures of higher symmetry, with unusual intermediate phases — incommensurate or *host-guest* structures — occurring along the way.

The computational study of the high-pressure behavior of materials necessitates the ability to properly examine displacive phase transitions from one structure to another. Some structural phase transitions are straightforward enough that the transition pressure can be determined by looking at where the enthalpy-pressure curves of the two structures cross, or by using the technique of the “common tangent” on the energy-volume curves of the two structures. However, the transition pressure cannot be determined in this way if the enthalpy-pressure (or energy-volume) curves of the two structures merge, as in the case of the A7 \rightarrow sc transition of arsenic (and for the same transition in the other group-V semi-metals). So if the phase transition between the two structures is a smooth one — such that the energy differences between the two structures in the region of the transition are extremely small — then how should such a transition be studied? High levels of convergence of the calculation of the quantities of interest are crucial.

In the past, the A7 \rightarrow sc transition pressure of arsenic has been the subject of experimental as well as theoretical dispute. Experimentally, there has been a long-standing question as to whether results obtained by Beister² for this transition pressure are correct over those of Kikegawa and Iwasaki³ — our results support

the findings of the former. Existing theoretical studies of arsenic yield a wide range of possible values for the transition pressure. We believe that a great part of the reason for this spread of values is inadequate k -point sampling of the Brillouin zone. The Fermi surface of arsenic is extremely complex: using values reported by Lin and Falicov⁴ for the cross-sectional area of a *neck* (the finest feature of the hole Fermi surface), we estimate that to sample the Fermi surface of arsenic at ambient pressures such that all of the features can be resolved — and are subsequently correctly weighted — a grid of at least $140 \times 140 \times 140$ k -points would be required. In practice, it is not necessary to use grids as dense as this but one would not know this without proper and thorough convergence testing with respect to k -point grid size and amount of smearing used. As no such convergence testing of the A7 \rightarrow sc transition of arsenic appears in the literature, results of computational studies to date are unreliable and any agreement with experiment has been fortuitous. We undertake indepth studies of the convergence properties of this transition,⁵ which enable us to proffer reliably converged results.

This investigation is not only timely, given the current levels of interest in the field of high-pressure research, but it is also especially relevant to the study of pressure-induced insulator to metal or semi-metal to metal phase transitions. In particular, we find that inspection of such transitions demands careful convergence of the quantities of interest with respect to k -point sampling and smearing, yet such testing is not always performed.

Using density functional theory (DFT) to study the high-pressure properties of materials furthermore necessitates an awareness of how different approximations to the exchange-correlation functional perform at such a task; to understand the differences encountered in the use of these functionals is in itself a motivation for undertaking

theoretical investigations of materials at high pressures.⁶ We thus compare the performance of the LDA with that of two GGA functionals, having achieved accurate results for each.

The paper is organized as follows. Section II contains the background material that pertains to our study, including a description of the A7 phase, a review of the structural transformation that yields the sc phase when a sufficiently high external pressure is applied, and a survey of the relevant findings published prior to this work. Section III deals with the computational details of our calculations. In Sec. IV, we present and discuss our results, contrasting them against those that appear in the literature. We begin by examining, using the nearest and next-nearest neighbor distances, the overall picture of the pressure-dependence of the phases of arsenic for the LDA and the GGA cases; the pressure-dependence of the lattice parameters is also explored. Next we focus on the A7 \rightarrow sc transition in particular, discussing it in more detail using energy-volume and pressure-volume curves. In Sec. V, we provide a brief discussion and conclusion.

II. THE STRUCTURES OF ARSENIC

At ambient pressures, arsenic is a covalently bonded compound existing in the rhombohedral (A7) phase. The A7 phase, belonging to space group 166, is a low-symmetry, three-fold coordinated, layered structure (Fig. 1). Nearest neighbors exist within a common layer; bonding between nearest neighbors gives the structure its buckled appearance. Adjacent layers, which contain next-nearest neighbors, are weakly bonded. The stacking of the layers occurs in the [111] direction, as does the buckling.

The rhombohedral primitive cell of arsenic contains two atoms and is described by the length of the primitive lattice vectors, a , the angle, α , between each set of primitive lattice vectors, and by the atomic positional parameter, z , which determines the positions of the two atoms along the cell's body diagonal. The two atoms are located at (Wyckoff) positions (z, z, z) and $(-z, -z, -z)$ ⁸ along the primitive lattice vectors, where the atomic positional parameter z is a fractional coordinate. Together, α and z characterize the degree of buckling experienced by the A7 structure.

The A7 structure can be interpreted as a distortion of the six-fold coordinated sc structure;^{9,10,11} a diagram charting the evolution of the sc structure into the A7 structure can be found in Ref. 2. The sc lattice can be viewed as being composed of two interpenetrating face-centered cubic (fcc) lattices. The vertices of a sc cell along the [111] direction contain one atom from each of the fcc lattices. A rhombohedral cell is superimposed onto this in such a way that its origin lies central to, and contains, two of these alternate fcc lattice atoms. Its body diagonal is along the [111] direction (the trigonal axis). Along this direction, the atomic positional param-

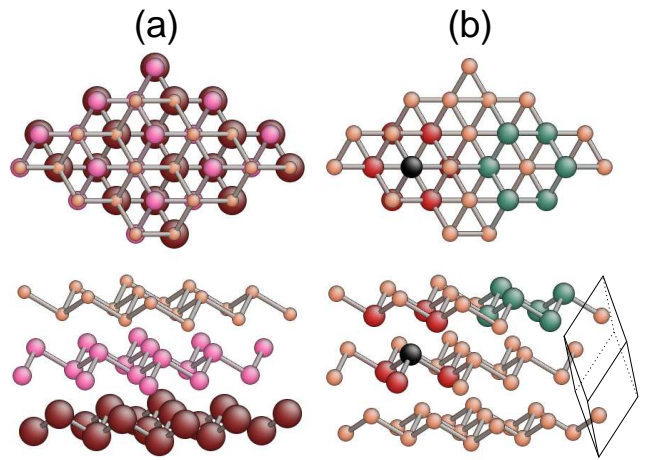


FIG. 1: (color online) The [111] direction is out of the page in the top portion of the figure; in the bottom portion of the figure it lies in the plane of the page and points upward. (a) Sizes and colors of atoms depicted carry no significance, but are employed merely to illustrate the ABC stacking of the A7 structure of arsenic. (b) The A7 structure consists of layers of 6-member buckled rings as displayed by the hexagon composed of green arsenic atoms. The buckled appearance of arsenic is due to the bonding of nearest neighbors that occurs within each of the layers; the layers themselves are only weakly bonded. Nearest and next-nearest neighbor distances are illustrated using the red atoms and are measured with respect to the black atom. Nearest neighbor distances exist between red and black atoms within the same layer; next-nearest neighbor distances exist between red and black atoms from adjacent layers. The two-atom rhombohedral unit cell is also displayed. (This figure was created in part using AtomEye.⁷)

eter z can be thought of as the ratio of the distance from the origin to the first atom, divided by the length of the body diagonal. A shear is then applied along the trigonal axis so that the angle α between sets of primitive lattice vectors decreases from its simple cubic value of 60° . Finally, the two atoms are displaced from their original positions and away from each other such that z decreases from its sc value of 0.25. The periodicity of the atoms in the [111] direction is now doubled; pairs of atoms in this direction repeat a pattern of being further apart and then nearer. In this way, the coordination number is reduced from six to three, as is consistent with the tendency of group-V semi-metals at normal pressures to form three bonds.

Subjected to sufficiently high pressures, arsenic undergoes a transition from semi-metallic A7 to metallic sc. At lower pressures, the stability of the A7 structure against that of the sc structure can be understood in terms of a Peierls-type distortion associated with the displacement of the atoms along the [111] direction from their original positions within the simple cubic lattice. This displacement corresponds to the longitudinal acoustic phonon mode at the point $R = \pi(1, 1, 1)/a$ on the boundary

of the simple cubic Brillouin zone.¹² The breaking of symmetry causes a lowering of the energy of the electron states near the Fermi level, with the result that a gap is opened up, the band contribution to the total energy is reduced, and the structure is stabilized against the distortion. As the pressure is increased, ionic effects become more significant, and the Ewald contribution to the total energy increases. Changes in the Ewald energy eventually dominate over changes in the band energy, the A7 structure is destabilized such that the Ewald energy is lowered, and the sc structure is recovered.^{10,12} Within the framework of chemical bonding, at low pressures the nearly orthogonal bonds of the A7 structure indicate weak s-p hybridization, where valence electrons are localized within saturated covalent bonds. The splitting between s and p bands increases with pressure, until the s band is so deeply depressed with respect to the p band that unsaturated orthogonal bonds form, resulting in the metallic sc structure.^{11,13}

It is sometimes convenient to use the nonprimitive hexagonal (trigonal) representation of the unit cell of arsenic. The trigonal cell is described by the lattice vectors \mathbf{a}_{hex} and \mathbf{c}_{hex} , the trigonal axis which lies in the [111] direction and coincides with the body diagonal of the rhombohedral primitive cell, and by the same atomic positional parameter z . The six atoms contained within the cell are located at Wyckoff positions $\pm(0, 0, z)rh$.⁸ The lattice vector lengths a_{hex} and c_{hex} are related to the length of the primitive lattice vector a and angle α as follows: $a_{\text{hex}} = 2a \sin(\alpha/2)$, and $c_{\text{hex}} = a\{3[1 + 2 \cos(\alpha)]\}^{1/2}$. Within this representation, z can be thought of as locating, as a fraction of \mathbf{c}_{hex} , the first atom from the origin along this axis.

From ambient conditions and with increasing pressure, the experimentally observed transition sequence for the phases of arsenic is A7 \rightarrow sc \rightarrow As-III \rightarrow bcc, where bcc is the body-centered cubic phase and As-III is an incommensurate structure. In the literature, the values reported for the pressure at which occurs the first structural transition of arsenic, from semi-metallic rhombohedral to metallic simple cubic, are spread out over a range of approximately 20 GPa. It has been theoretically predicted that arsenic should undergo a structural phase transition at 18 GPa;¹⁴ early numerical studies of arsenic yielded for the transition pressure values of 35 GPa¹² and 19 GPa.¹¹ This last result corresponded to $V/V_0 \simeq 0.8$ (and was indeed found again very recently in a study of the lattice dynamics of arsenic to be the volume ratio at which a transition occurs¹⁵), where V is the volume of the compressed cell and V_0 is the uncompressed equilibrium volume. Investigating the pressure-induced superconductivity of arsenic, the experimental findings of Kawamura and Wittig¹⁶ suggest a transition at 24 GPa, while those of Chen, *et al.*¹⁷ support a transition pressure of 32 GPa, though they obtain 36 GPa via the theoretical component of their study. Performing energy-dispersive and angle-dispersive powder X-ray diffraction studies of arsenic up to 45 GPa, Kikegawa

and Iwasaki³ determined the A7 \rightarrow sc transition to be of first order, occurring somewhere in the interval of 31.4–36.6 GPa and resulting in a cell volume discontinuity of $\Delta V/V_T \simeq 5\%$, where ΔV is the difference in the cell volume across transition, and V_T is the volume of the cell just prior to the transition. Beister, *et al.*,² conducting an angle-dispersive powder X-ray diffraction study up to 33 GPa in addition to a Raman investigation, concluded that the transition occurs at 25 GPa, and that to within their experimental uncertainty no discernable change in volume is seen to occur: $\Delta V/V_T < 0.5\%$. More recently, theoretical investigations of the A7 \rightarrow sc transition of arsenic yielded for the transition pressure a range of 25 ± 8 GPa¹⁸ in one study, and 28 GPa¹⁹ in another. A molecular dynamics simulation of the A7 \rightarrow sc transition performed by Durandurdu²⁰ yielded a transition pressure of 35 GPa and a volume discontinuity of 3.2%, and most recently, transition pressures of 22 GPa²¹ and 26.3 GPa²² have been found, with volume discontinuities of 0.8% and 0.4% respectively.

Experiments aimed at investigating the higher-pressure phase transitions of arsenic were first carried out by Greene, *et al.*²³ Energy-dispersive powder X-ray diffraction experiments on arsenic up to 122 GPa yielded sc \rightarrow As-III and As-III \rightarrow bcc transition pressures of 48 ± 11 GPa and 97 ± 14 GPa, respectively. To within their experimental error of 1%, no measurable volume discontinuities for either phase transition were observed. These results were reproduced rather closely in a theoretical study by Häussermann, *et al.*,¹⁹ in which the two pressures were found to be 43 GPa and 97 GPa. Reinterpretation of diffraction patterns obtained in the experiments of Greene, *et al.* led Iwasaki²⁴ (see also Ref. 25) to suggest a tetragonal Bi-III-type or Sb-II-type structure, regarded as distorted bcc, for the As-III phase. More recently McMahon, *et al.*,²⁶ using angle-dispersive X-ray diffraction techniques, determined both the Bi-III and Sb-II phases to be Ba-IV-type structures, consisting of a body-centered tetragonal (bct) *host* structure containing a bct *guest* component that is incommensurate with the host along the tetragonal c axis. They suggested that a modification of this structure in which the host component is bct and the guest is monoclinic would be appropriate for As-III. Degtyareva, *et al.*²⁷ later found that the As-III structure closely resembles that of Sb-IV, and proposed that it is possible that arsenic may undergo an incommensurate-to-incommensurate transition between the As-III and bcc phases similar to the Sb-IV \rightarrow Sb-II transition observed in their study.

III. COMPUTATIONAL DETAILS

All calculations were performed using the CASTEP code.²⁸ For the exchange-correlation functional, we use the local density approximation (LDA)²⁹ as parametrized by Perdew and Zunger,³⁰ the Perdew-Burke-Ernzerhof generalized gradient approximation (abbreviated as

GGA-PBE)³¹ and the Perdew-Wang generalized gradient approximation (GGA-PW91).³²

The interaction between the core and valence states of arsenic is described using scalar-relativistic ultra-soft pseudopotentials.³³ For the calculations to proceed efficiently, such pseudopotentials require the use of two FFT-grids: a *standard* grid, which is used to represent the pseudo wave-functions, and a *fine* grid, which is used to store the charge density, and thus the ultra-soft augmentation charge. The size of the standard grid is determined by the *cut-off energy* — the maximum energy accounted for in the plane-wave expansion of the wave-functions; the fine grid must be chosen dense enough such that the charge-density within the atomic cores is reproduced with sufficient detail — this is a requirement to ensure well-converged forces and stresses. Convergence tests on our system at atmospheric pressure led us to choose a cut-off energy of 450 eV; we chose our fine grid to be twice as dense as our standard grid. With these choices, our energies, forces and stresses are converged to within 0.003 eV/atom, 0.001 eV/Å and 0.01 GPa, respectively.

We apply pressures between 0 GPa and 200 GPa to the two-atom rhombohedral unit cell of arsenic, allowing cell lengths and angles in addition to atomic positions to vary. For each applied pressure, the enthalpy is minimized such that the system is relaxed from the structure that exists at atmospheric pressure as determined experimentally by Schiferl.³⁴ The geometry optimizations are made to continue until the differences in the forces and stresses between iterations are less than 0.005 eV/Å and 0.05 GPa, respectively. Proper convergence studies in electronic structure calculations are important and the lack of such testing can lead to severe inaccuracies.³⁵ Accordingly, we have thoroughly investigated the structural convergence of our system in the region of the A7 → sc phase transition; we have examined the convergence with respect to k -point grid size and amount of cold-smearing³⁶ used — the results of this convergence testing can be found in the supplementary material provided.⁵ In the vicinity of the A7 → sc transition, the k -point grids that have been studied are $n \times n \times n$, where n is 24, 25, 26, 33, 50 and 66 (all k -point grids are unshifted, so that the gamma point has been included in the calculations), using cold-smearings of 0.1, 0.2 and 0.5 eV in the LDA and 0.1 eV in the GGA-PBE. At pressures outside the region of this phase transition (and for all pressures studied in the case of the GGA-PW91), a k -point grid of $33 \times 33 \times 33$ is used, along with a cold-smearing of 0.1 eV. The symmetry of the initial A7 structure is maintained throughout the relaxation, as a highly symmetric path is assumed for the A7 → sc transition, with atoms moving only along the [111] direction. Although it is irrelevant whether this assumption is valid for the As-III phase, because no attempt has been made here to properly model this incommensurate structure, it seems reasonable that imposing these constraints on the symmetry of the system will not affect the transi-

tion pressures observed since the incommensurate phase is bounded by two phases of higher symmetry than the original A7 structure.

Finally, all calculations are performed at $T = 0$ K, and the zero-point vibrational energy, as well as the spin-orbit interaction, are neglected.

IV. RESULTS AND DISCUSSION

A. Overview of the transitions of arsenic

We first take an overview of the behavior of the nearest and next-nearest neighbor distances as the pressure is increased from 0 GPa to 200 GPa. It has already been stated that for the A7 → sc phase transition in particular, the behavior of these two quantities gives the clearest indication of when a structural phase transition has occurred. Fig. 2 reveals the results we obtained for each of the exchange-correlation functionals studied, and includes separate close-ups of the A7 → sc phase transition for the LDA and for the GGA. Indeed, it is quite clear when this transition occurs in all cases, as it happens when the nearest and next-nearest neighbor distances become equal. From the insets of Fig. 2, we can conclude that the A7 → sc phase transition of arsenic occurs at 21 ± 1 GPa in the LDA, at 28 ± 1 GPa in the GGA-PBE and at 29 ± 1 GPa in the GGA-PW91 (note that the difference in the transition pressure that arises from the use of the GGA-PW91 over the GGA-PBE is negligible as it is within the uncertainty of 1 GPa). This result is more consistent with the experimental findings of Beister, *et al.*,² who found the phase transition to occur at 25 ± 1 GPa, than it is with those of Kikegawa and Iwasaki,³ who found it to occur in the range of 31.4–36.6 GPa; it furthermore disagrees with the outcome of simulations performed recently by Durandurdu.²⁰

From this same figure we note incidentally that the GGA nearest and next-nearest neighbor distances are always larger than those resulting from the LDA. This is due to the well-known fact that the LDA tends to overbind systems, whereas the GGA tends to underbind them.³⁷ Thus cell volumes, cell parameters, and distances contained within the cell will tend to be lower for the LDA than for the GGA.

Our unit cell contains two atoms and is periodically repeated. We cannot hope to say anything about the incommensurate phase that occurs in the pressure-induced progression of phases of arsenic, and it is not our intention to do so in this paper; to acknowledge this point, we will use the abbreviation *incomm.* to represent what we find between the sc and bcc phases, and subsequently write the progression of phases as A7 → sc → *incomm.* → bcc. We mention as an aside that we have chosen to work with the two-atom unit cell of arsenic in the interest of undertaking efficient calculations, but as we are guided by experiment and not

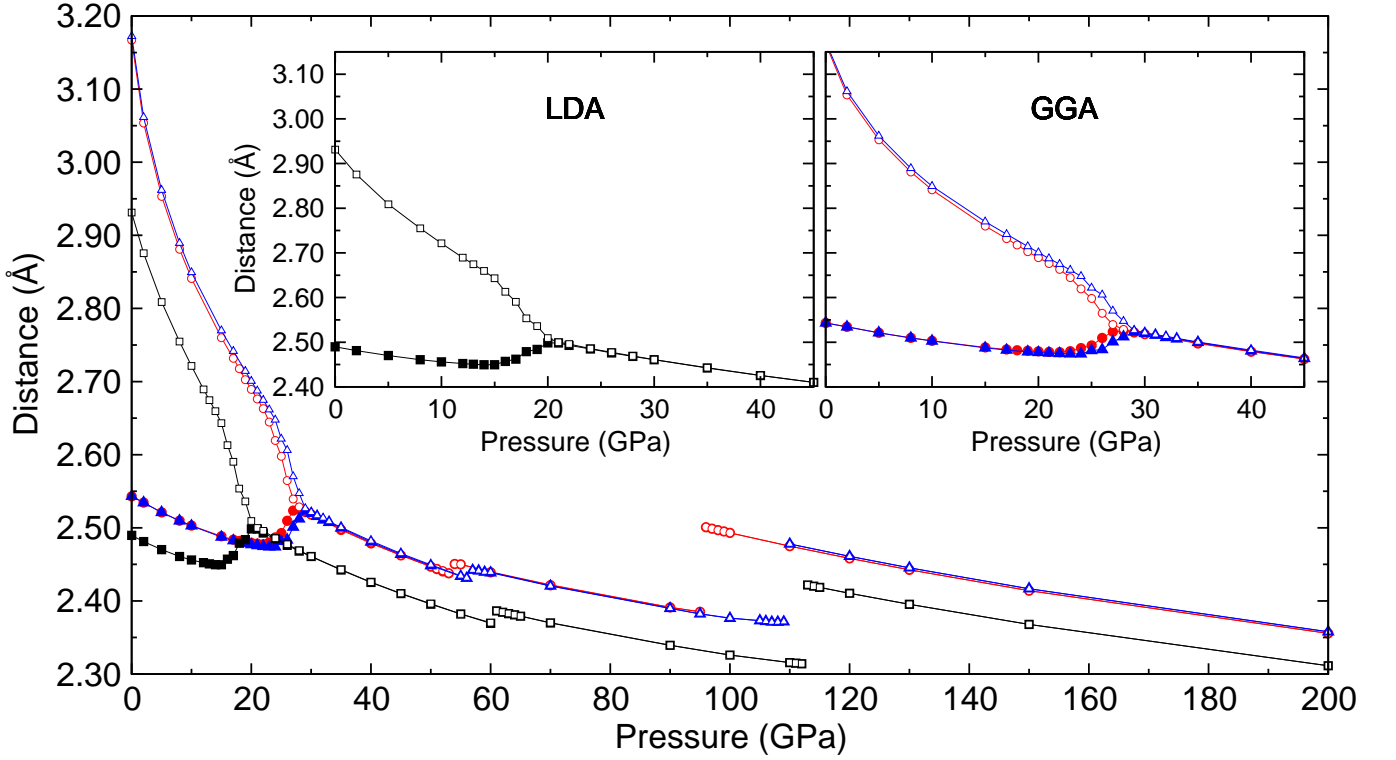


FIG. 2: (color online) Nearest neighbor (solid symbols) and next-nearest neighbor (open symbols) distances as a function of pressure for the LDA (black squares), for the GGA-PBE (red circles) and for the GGA-PW91 (blue triangles). The $A7 \rightarrow sc$, $sc \rightarrow incomm.$ and $incomm. \rightarrow bcc$ transitions are evident, where the insets emphasize the $A7 \rightarrow sc$ transition in both the LDA and the GGA. (Calculations performed using a $33 \times 33 \times 33$ k -point grid and a cold-smearing of 0.1 eV.)

primarily focused in this study on the incommensurate structure, a two-atom unit cell is sufficient for our needs. It is possible that were we to use unit cells containing arbitrary numbers of atoms we might discover other more complex or more closely-packed structures of arsenic at pressures higher than have yet been attained experimentally — this is an interesting point and although outside the scope of this work, would be an excellent candidate for the application of fully randomized structure prediction.³⁸

Having stated that we do not expect to reproduce the incommensurate phase of arsenic, we can still use our system to approximate the pressure at which the system ceases to be sc , as well as to approximate the pressure at which it becomes bcc , and compare with the most recent experimental findings. Thus, referring again to Fig. 2, we see that in the LDA the $sc \rightarrow incomm.$ phase transition appears to occur at 60–61 GPa and the $incomm. \rightarrow bcc$ at 112–113 GPa. In the GGA-PBE it is 53–54 GPa and 95–96 GPa, and in the GGA-PW91 it is 56–57 GPa and 109–110 GPa. Although our findings for the $sc \rightarrow incomm.$ transition are about 10 GPa higher than those of Ref. 19, and fall into the high-end of the range of values given in Ref. 23, our results for the $incomm. \rightarrow bcc$ transition agree closely with those from both works. Along with the findings that are present in the literature, our

results for the transition pressures of arsenic are summarized in Table I.

We break down the nearest and next-nearest neighbor distances into their constituent components in Fig. 3, which illustrates the behavior of the lattice parameter a (top tier), the cell angle α (middle tier), and the atomic positional parameter z (bottom tier), for the LDA and the GGA-PBE. Each tier of Fig. 3 is composed of a close-up of the $A7 \rightarrow sc$ phase transition (on the left) along with the behavior of the quantity over the entire range of pressures studied (on the right). Respectively, the high symmetry values of α and z , as can be confirmed in this figure, are 60° and 0.25 in the simple cubic case, and 90° and 0.25 in the bcc case. The sc phase is of higher symmetry than the $A7$ phase, and because we have constrained the symmetry of the system, once the sc phase has been reached the atomic positional parameter z remains equal to 0.25. Thus, after the $A7 \rightarrow sc$ phase transition has occurred, it is the angle α that determines the phase of the structure as the applied pressure is increased.

The first point to observe upon inspection of Fig. 3 is that the $A7 \rightarrow sc$ transition appears to be continuous with respect to all three quantities: a (top), α (middle) and z (bottom). We see from the set of right hand panels in the figure that the $sc \rightarrow incomm.$ and the $incomm. \rightarrow bcc$ transitions appear to be discontinuous with

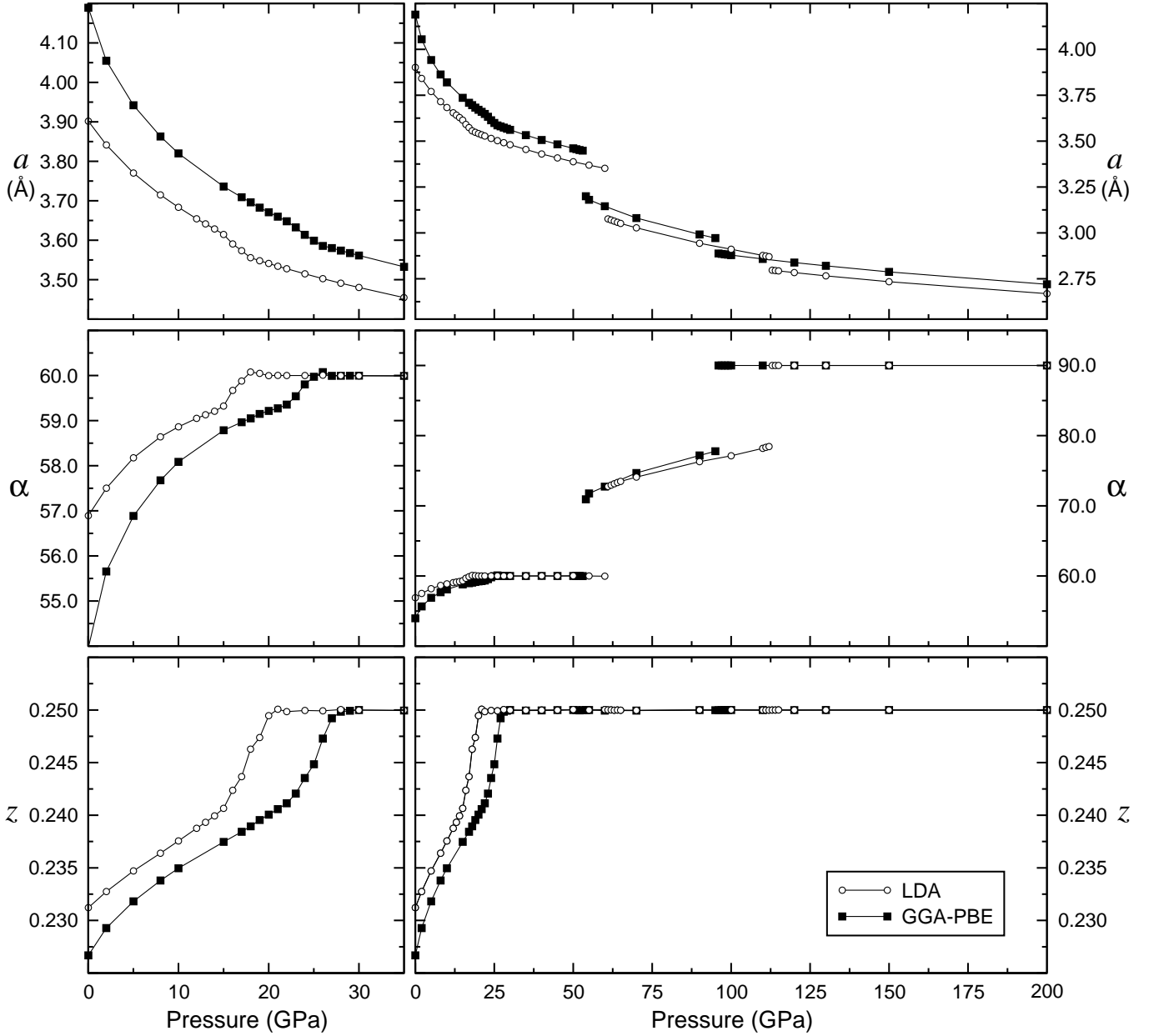


FIG. 3: Lattice parameter a (top tier), cell angle α (middle tier) and atomic positional parameter z (bottom tier) as a function of pressure for the LDA (open circles) and for the GGA-PBE (filled squares). The left-hand panels emphasize the A7 \rightarrow sc transition, while in addition the sc \rightarrow *incomm.* and *incomm.* \rightarrow bcc transitions are apparent in the top two tiers of the right-hand panels. (Calculations performed using a $33 \times 33 \times 33$ k -point grid and a cold-smearing of 0.1 eV.)

respect to lattice parameter a and cell angle α , for both the LDA and the GGA; in particular, these discontinuities subsequently manifest themselves in the nearest and next-nearest neighbor distances at these two transitions as can be seen in Fig. 2, and indicate when the cell angle has jumped away from 60° in the case of the former transition, and to 90° in the case of the latter. Before discussing the behavior with pressure of the cell parameters further, we first inspect more closely the A7 \rightarrow sc transition.

B. The A7 \rightarrow sc transition of arsenic

Examining the left hand panels of Fig. 3, we see that α and z reach their high-symmetry values at lower pressures in the case of the LDA than in the GGA; this is to be expected as we noted earlier that the LDA A7 \rightarrow sc transition pressure is lower than the GGA transition pressure. However, we also note that in both cases, α reaches 60° at a slightly lower pressure than z reaches 0.25. This result was also found by

TABLE I: Transition pressure P_T , reduced transition volume V_T/V_o , where V_T is the volume just prior to the transition and V_o is the uncompressed equilibrium volume, and percentage volume change across the A7 \rightarrow sc transition. Below are listed transition pressures for the higher pressure transitions of arsenic. Parametrizations of the generalized gradient approximation to the exchange-correlation functional that appear below are PBE³¹ and PW91.³² (Abbreviations: PP – pseudopotential approach, LAPW – linear augmented plane wave approach.)

A7 \rightarrow sc	P_T (GPa)	V_T/V_o	$\Delta V/V_T$ (%)
Theory:			
This work, LDA	21 ± 1		
This work, PBE	28 ± 1		
This work, PW91	29 ± 1		
Ref. 12 (PP, LDA)	35	0.72	
Ref. 11 (LAPW, LDA)	19	0.8	
Ref. 17 (PP, LDA)	36		
Ref. 18 (PP, LDA)	25 ± 8	0.78	1
Ref. 19 (PP, PW91)	28		0.8
Ref. 20 (PP, LDA)	35		3.2
Ref. 21 (PP, PBE)	22		0.8
Ref. 15 (PP, PW91)		0.8	
Ref. 22 (LAPW, PBE)	26.3		0.4
Experiment:			
Ref. 14	18		
Ref. 16	24		
Ref. 3	$31.4 - 36.6$	0.744	5
Ref. 2	25 ± 1	0.772	0.5
Ref. 17	32		
P_T (GPa)	sc \rightarrow incomm.	incomm. \rightarrow bcc	
Theory:			
This work, LDA	60.5 ± 0.5	112.5 ± 0.5	
This work, PBE	53.5 ± 0.5	95.5 ± 0.5	
This work, PW91	56.5 ± 0.5	109.5 ± 0.5	
Ref. 19 (PP, PW91)	43	97	
Experiment:			
Ref. 23	48 ± 11	97 ± 14	

Seifert, *et al.*³⁷ in their study of the A7 \rightarrow sc transition of antimony. In fact, there is no reason to assume that α and z must reach their high-symmetry values at the same pressure — yet we cannot rule out the possibility that this pressure discrepancy may be an artifact resulting from the use of smearing in our calculations. The difference in pressures between which α and z reach their high-symmetry values is slightly more pronounced for the LDA (approximately 3 GPa) than it is for the GGA (approximately 2 GPa for both the GGA-PBE and the GGA-PW91). The curves of the lattice parameter a and the cell angle α seemingly progress together. Thus the cell reaches its high-symmetry shape “before” the transition to sc takes place; since both α and z must reach their high-symmetry values for the transition to occur, the A7 \rightarrow sc transition pressure is consequently determined by the atomic positional parameter z . Thus we see that z reaches 0.25 at approximately 21 GPa in the LDA and at approximately 28 GPa in the GGA-PBE.

We consider next, for the LDA and the GGA-PBE, the energy-volume and pressure-volume curves of the A7 and sc structures over a pressure range of approximately 0–45 GPa, which includes only the A7 \rightarrow sc phase transition (Fig. 4). In all cases, the A7 and sc curves merge once the A7 \rightarrow sc phase transition has occurred, in other words, once the volume of the cell has been compressed beyond a particular value. This contradicts the recent results of Durandurdu.²⁰ However, the sc \rightarrow A7 transformation is the result of two continuous distortions, so we would expect this transition also to be smooth and continuous. We do not expect to see metastable states, and we observe none — this agrees with the experimental findings both of Beister, *et al.*,² and of Kikegawa and Iwasaki,³ yet it disagrees with the theoretical findings of Da Silva, *et al.*¹⁸ We observe no discontinuities in these curves and so our results suggest that the A7 \rightarrow sc phase transition is of second order. Experimentally, both Beister, *et al.*² and Kikegawa and Iwasaki³ report that the A7 \rightarrow sc transition is of first order, where to within an experimental error of 0.5% no volume discontinuity is detected in the former study, whereas a volume discontinuity of 5% across the transition is found in the latter study. Da Silva, *et al.*¹⁸ report a transition that is weakly first order, and a volume discontinuity of less than 1%. We believe that if this transition appeared in the past to be of first order it was because of the coarse grained nature of the investigations performed at the time.

On the matter of the discrepancies that exist between our study and, for example, those of Durandurdu²⁰ and Da Silva, *et al.*,¹⁸ it is clear that in those investigations the k -point sampling of the Brillouin zone was insufficient: the most dense grid employed by Da Silva, *et al.*¹⁸ in their study of arsenic was $13 \times 13 \times 13$ — Durandurdu²⁰ uses only the gamma point for a unit cell containing 250 atoms, roughly corresponding to using a $5 \times 5 \times 5$ k -point grid for a two-atom unit cell. Our investigations reveal that these calculations could not have been converged. Moreover, in addition to ensuring that the Brillouin zone is properly sampled, we believe that choosing an appropriate amount of smearing is also very important (once again consult the supplementary material for an indepth study of the convergence properties with respect to k -point sampling and smearing of the A7 \rightarrow sc transition of arsenic).⁵

Another point to be made about the insets of Fig. 2, is that at pressures just below the A7 \rightarrow sc transition, the nearest neighbor distance actually increases with pressure. This occurs over the range of approximately 15–20 GPa in the LDA and approximately 22–27 GPa in the GGA-PBE. The onset of this feature coincides with the point at which the a , α and z versus pressure curves all begin to experience a kink or slight change of direction (see left-hand panels of Fig. 3). These pressure intervals also correspond to the regions where the A7 pressure-volume curves of Fig. 4 start dipping down (from right to left) toward those of the simple cubic phase. As the volume does not increase discontinuously across the tran-

sition, there must be significant atomic restructuring going on for the nearest neighbor distance to increase as the transition is approached. Although their nearest and next-nearest neighbor distances were estimates calculated according to an empirical relation for the atomic positional parameter, Beister, *et al.*² noticed this point as well and noted that such behavior is not unexpected, as there is a tendency in covalently bonded solids to display increased nearest neighbor distances when undergoing pressure-induced breaking of directional bonds, accompanied by increased coordination numbers.

We have performed fits of the energy-volume curves using both the third-order Birch-Murnaghan³⁹ and Vinet⁴⁰ equations to yield values for the bulk modulus, B_o , pressure derivative of the bulk modulus, B'_o , and equilibrium volume, V_o , of arsenic for both the A7 and sc structures. We find that for the A7 phase, the values we obtain for B_o and B'_o are extremely sensitive to the number of points included in the fit; this was also found to be the case for Needs, *et al.*¹⁰ It is also somewhat the case for the sc portion of the A7 curve, so we have quoted the values that we obtain when we fit curves resulting from compressions of the exact sc structure, rather than from geometry optimizations. Table II summarizes our findings, including the results we obtained for the equilibrium cell parameters from our geometry optimizations of arsenic at zero pressure, and compares them to those published in previous studies.

V. CONCLUSIONS

We have performed simulations of the two-atom unit cell of arsenic under compression to investigate its high-

pressure behavior and compare with experiment. In the matter of the A7 \rightarrow sc transition, our results strongly support the experimental findings of Beister² over those of Kikegawa and Iwasaki;³ we furthermore find this transition to be of second order.

Our main critique of the current literature is that we believe that any results published until now concerning this semi-metal to metal phase transition are unconverged (as no thorough convergence studies have ever been published), and that any agreement with experiment has merely been fortuitous. This study has enabled us to present reliably converged results for the A7 \rightarrow sc transition of arsenic.

Using DFT to study any pressure-induced structural phase transition involving a metal demands convergence testing similar to that which we have carried out;⁵ for such purposes, k -point sampling and smearing must be considered thoroughly.

VI. ACKNOWLEDGMENTS

We thank Richard Needs for helpful discussions. Computing resources were provided by the Cambridge High Performance Computing Service (HPCS).

-
- ¹ M. I. McMahon and R. J. Nelmes, *Chem. Soc. Rev.* **35**, 943 (2006).
 - ² H. J. Beister, K. Strössner, and K. Syassen, *Phys. Rev. B* **41**, 5535 (1990).
 - ³ T. Kikegawa and H. Iwasaki, *J. Phys. Soc. Jpn.* **56**, 3417 (1987).
 - ⁴ P. J. Lin and L. M. Falicov, *Phys. Rev.* **142**, 441 (1966).
 - ⁵ See EPAPS Document No. [...] for the convergence properties of the A7 \rightarrow sc phase transition. For more information on EPAPS, see <http://www.aip.org/pubservs/epaps.html>.
 - ⁶ A. Mujica, A. Rubio, A. Muñoz, and R. J. Needs, *Rev. Mod. Phys.* **75**, 863 (2003).
 - ⁷ J. Li, *Modelling Simul. Mater. Sci. Eng.* **11**, 173 (2003).
 - ⁸ R. W. G. Wyckoff, *Crystal Structures*, vol. 1 (John Wiley & Sons, Inc., New York, 1963), 2nd ed.
 - ⁹ L. M. Falicov and S. Golin, *Phys. Rev.* **137**, A871 (1965).
 - ¹⁰ R. J. Needs, R. M. Martin, and O. H. Nielsen, *Phys. Rev. B* **33**, 3778 (1986).
 - ¹¹ L. F. Mattheiss, D. R. Hamann, and W. Weber, *Phys. Rev. B* **34**, 2190 (1986).
 - ¹² K. J. Chang and M. L. Cohen, *Phys. Rev. B* **33**, 7371 (1986).
 - ¹³ P. B. Littlewood, *J. Phys. C* **13**, 4855 (1980).
 - ¹⁴ J. E. Schirber and J. P. Van Dyke, *Phys. Rev. Lett.* **26**, 246 (1971).
 - ¹⁵ S. Shang, Y. Wang, H. Zhang, and Z.-K. Liu, *Phys. Rev. B* **76**, 052301 (2007).
 - ¹⁶ H. Kawamura and J. Wittig, *Physica B* **135**, 239 (1985).
 - ¹⁷ A. L. Chen, S. P. Lewis, Z. Su, P. Y. Yu, and M. L. Cohen, *Phys. Rev. B* **46**, 5523 (1992).
 - ¹⁸ C. R. S. Da Silva and R. M. Wentzcovitch, *Comput. Mater. Sci.* **8**, 219 (1997).
 - ¹⁹ U. Häussermann, K. Söderberg, and R. Norrestam, *J. Am. Chem. Soc.* **124**, 15359 (2002).
 - ²⁰ M. Durandurdu, *Phys. Rev. B* **72**, 073208 (2005).
 - ²¹ W. Feng, S. Cui, H. Hu, and H. Liu, *Physica B* **400**, 22 (2007).
 - ²² E. S. Zijlstra, N. Huntemann, and M. E. Garcia, *New J. Phys.* **10**, 033010 (2008).
 - ²³ R. G. Greene, H. Luo, and A. L. Ruoff, *Phys. Rev. B* **51**, 597 (1995).
 - ²⁴ H. Iwasaki, *Phys. Rev. B* **55**, 14645 (1997).
 - ²⁵ H. Iwasaki and T. Kikegawa, *Acta Crystallogr. Sect. B* **53**, 353 (1997).

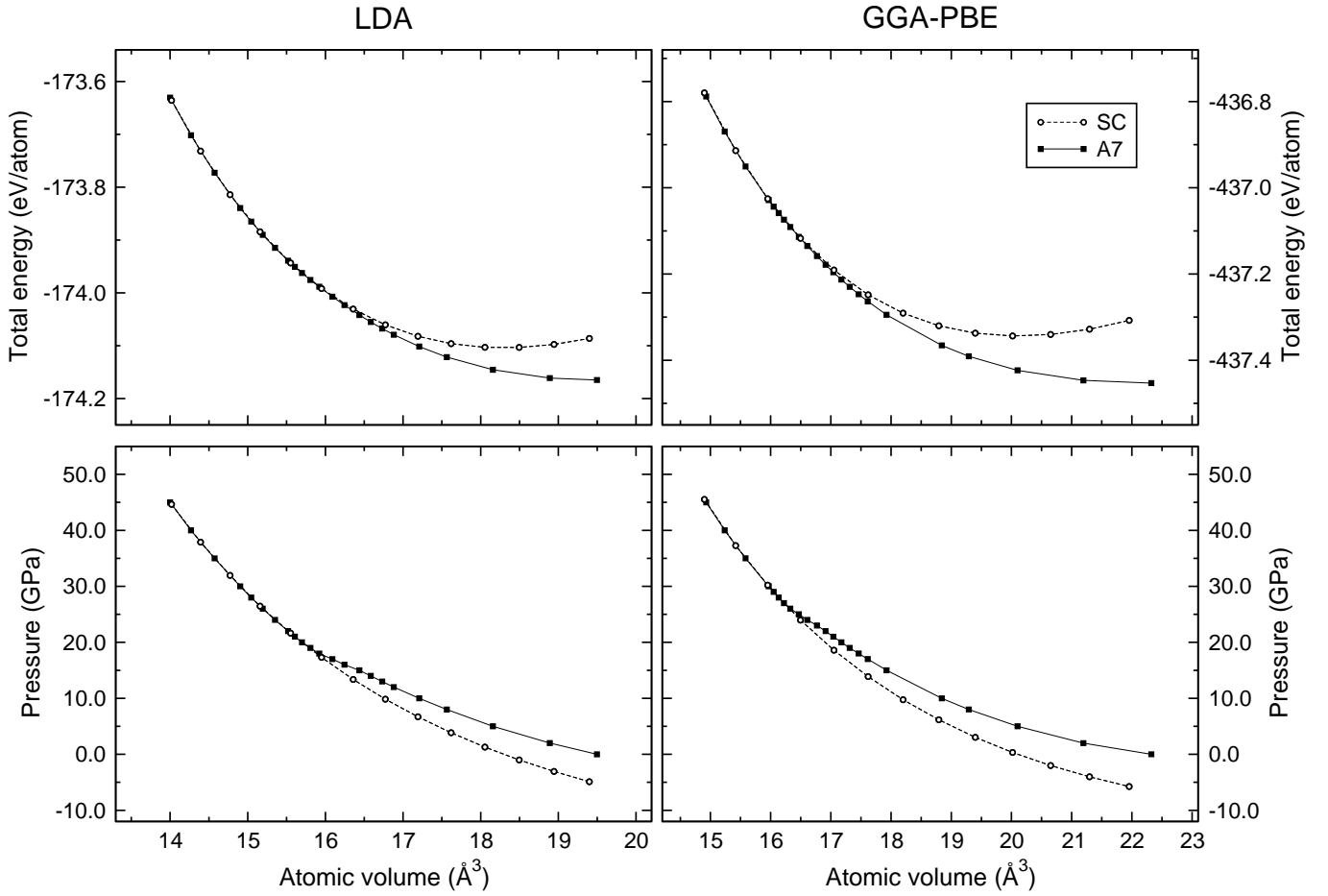


FIG. 4: Energy-volume (top) and pressure-volume (bottom) curves of the A7 phase (filled squares) and of the simple cubic phase (open circles) for the LDA (left) and for the GGA-PBE (right). For each of the four plots, the A7 and simple cubic curves merge, and there are no discontinuities present suggesting that the A7 \rightarrow sc transition of arsenic is of second order. (Calculations performed using a $33 \times 33 \times 33$ k -point grid and a cold-smearing of 0.1 eV.)

- ²⁶ M. I. McMahon, O. Degtyareva, and R. J. Nelmes, Phys. Rev. Lett. **85**, 4896 (2000).
- ²⁷ O. Degtyareva, M. I. McMahon, and R. J. Nelmes, Phys. Rev. B **70**, 184119 (2004).
- ²⁸ S. J. Clark, M. D. Segall, C. J. Pickard, P. J. Hasnip, M. J. Probert, K. Refson, and M. C. Payne, Z. Kristallogr. **220**, 567 (2005).
- ²⁹ D. M. Ceperley and B. J. Alder, Phys. Rev. Lett. **45**, 566 (1980).
- ³⁰ J. P. Perdew and A. Zunger, Phys. Rev. B **23**, 5048 (1981).
- ³¹ J. P. Perdew, K. Burke, and M. Ernzerhof, Phys. Rev. Lett. **77**, 3865 (1996).
- ³² J. P. Perdew and Y. Wang, Phys. Rev. B **45**, 13244 (1992).
- ³³ D. Vanderbilt, Phys. Rev. B **41**, 7892 (1990).
- ³⁴ D. Schiffrer and C. S. Barrett, J. Appl. Crystallogr. **2**, 30 (1969).
- ³⁵ M. J. Mehl, Phys. Rev. B **61**, 1654 (2000).
- ³⁶ N. Marzari, D. Vanderbilt, A. De Vita, and M. C. Payne, Phys. Rev. Lett. **82**, 3296 (1999).
- ³⁷ K. Seifert, J. Hafner, J. Furthmüller, and G. Kresse, J. Phys.: Condens. Matter **7**, 3683 (1995).
- ³⁸ C. J. Pickard and R. J. Needs, Phys. Rev. Lett. **97**, 045504 (2006).
- ³⁹ F. Birch, Phys. Rev. **71**, 809 (1947).
- ⁴⁰ P. Vinet, J. R. Smith, J. Ferrante, and J. H. Rose, Phys. Rev. B **35**, 1945 (1987).
- ⁴¹ J. P. Perdew and Y. Wang, Phys. Rev. B **33**, 8800 (1986).
- ⁴² J. P. Perdew, Phys. Rev. B **33**, 8822 (1986).
- ⁴³ A. D. Becke, Phys. Rev. A **38**, 3098 (1988).
- ⁴⁴ R. J. Needs, R. M. Martin, and O. H. Nielsen, Phys. Rev. B **35**, 9851 (1987).
- ⁴⁵ B. Morosin and J. E. Schirber, Solid State Commun. **10**, 249 (1972).

TABLE II: Lattice parameters for the uncompressed arsenic structure (A7), in addition to the equilibrium volume (V_o), bulk modulus (B_o) and pressure derivative of the bulk modulus (B'_o). Those for the uncompressed simple cubic structure of arsenic are listed further below. Parametrizations of the generalized gradient approximation to the exchange-correlation functional that appear below are PBE,³¹ PW86⁴¹ and PB.^{42,43} (Abbreviations: PP – pseudopotential approach, LAPW – linear augmented plane wave approach, BM – fitted with the third order Birch-Murnaghan³⁹ equation, V – fitted with the Vinet⁴⁰ equation.)

A7 structure	a (Å)	α (°)	z	V_o (Å ³)	B_o (GPa)	B'_o
Theory:						
This work, LDA	3.902	56.89	0.231	19.48(1) ^{BM,V}	60.9(1.6) ^{BM,V}	4.6(4) ^{BM} , 4.8(4) ^V
This work, PBE	4.189	53.96	0.227	22.22(5) ^{BM,V}	36.9(1.6) ^{BM,V}	6.1(7) ^{BM} , 6.25(55) ^V
This work, PW91	4.195	53.90	0.227	22.30(2) ^{BM,V}	36.9(1.6) ^{BM,V}	6.2(5) ^{BM} , 6.3(4) ^V
Ref. 10 (PP, LDA)	4.017	56.28	0.230	20.95	43	
Ref. 44 (PP, LDA)			0.24			
Ref. 11 (LAPW, LDA)	4.084	55.9	0.2294	21.8	77	
Ref. 37 (PP, LDA)	4.0027	56.24	0.230	20.70	52	
(PP, PB)	4.32035	52.44	0.225	23.45	36	
(PP, PW86)	4.57449	52.01	0.224	27.49		
Ref. 18 (PP, LDA)	4.031	56.3	0.230	21.18	59(1)	4.2(3)
Ref. 20 (PP, LDA)				23.57	64.49	3.99
Ref. 21 (PP, PBE)	4.182	53.13	0.225	21.70	38.4	4.34
Ref. 22 (LAPW, PBE)	4.246	53.31	0.226	22.82		
Experiment:						
Ref. 34	4.1018(1)	55.554(1)	0.22764(4)	21.303		
Ref. 45			0.22728(7)			
Ref. 3	4.133	54.12	0.227	21.53	55.6	4.4
Ref. 2		54.13			58(4)	3.3(4)
Ref. 23					56(3)	3.7(2)
Simple cubic structure						
Simple cubic structure	a_{cub} (Å)			V_o (Å ³)	B_o (GPa)	B'_o
Theory:						
This work, LDA	2.635			18.30 ^{BM,V}	94.53(16) ^{BM} , 93.57(32) ^V	4.29(2) ^{BM} , 4.48(3) ^V
This work, PBE	2.719			20.10 ^{BM,V}	78.99(3) ^{BM} , 78.51(16) ^V	4.318(4) ^{BM} , 4.55(2) ^V
This work, PW91	2.722			20.17 ^{BM,V}	78.84(4) ^{BM} , 78.32(19) ^V	4.297(3) ^{BM} , 4.53(2) ^V
Ref. 10 (PP, LDA)	2.687			19.4	104	4.4
Ref. 44 (PP, LDA)	2.68			19.25	122	2.32
Ref. 11 (LAPW, LDA)	2.717			20.06	87	
Ref. 18 (PP, LDA)	2.704			19.77	92(3)	4.2(3)
Ref. 20 (PP, LDA)	2.822			22.47	74.15	3.2
Ref. 21 (PP, PBE)	2.674			19.12	88.2	3.93
Ref. 22 (LAPW, PBE)	2.731			20.37	78.107	4.317